SoftwareX 11 (2020) 100442

Contents lists available at ScienceDirect

SoftwareX

journal homepage: www.elsevier.com/locate/softx

Original software publication

Reaction Network Viewer (ReNView): An open-source framework for reaction path visualization of chemical reaction systems

Udit Gupta, Dionisios G. Vlachos *

Department of Chemical and Biomolecular Engineering, Rapid Advancement in Process Intensification Deployment (RAPID) Institute, Delaware Energy Institute, University of Delaware, Newark, DE 19716, USA

ARTICLE INFO

Article history:
Received 12 July 2019
Received in revised form 21 January 2020

Keywords:
Reaction flux analysis
Reaction path analysis
Visualization
Reaction network
Graph representation
Data compression

ABSTRACT

Reaction Path Analysis (RPA) is an essential tool in identifying the key reaction pathways that drive chemical transformations of complex reaction networks. In this work, an open-source, standalone reaction path visualizer has been developed for complex reaction systems. The reaction path visualizer generates a graphical representation of the reaction network based on reaction fluxes that enables identification of dominant reaction pathways and mechanism reduction. The visualizer generates network and species visualizations given the output of a microkinetic model. The python code employed for the visualizer can easily be integrated with any chemical kinetics solver. The efficacy of the visualizer is demonstrated through three case studies.

Code metadata

Current code version	v1.1
Permanent link to code	https://github.com/ElsevierSoftwareX/SOFTX_2019_239
Legal Code License	GNU Lesser GPL v3 license
Code versioning system used	Git
Software code languages, tools, and services used	Python, NumPy, Pandas, Graphviz, NetworkX, Anaconda
Operating environments	Mac/Linux/Windows
If available Link to developer documentation/manual/examples	https://github.com/VlachosGroup/ReNView/wiki
Support email for questions	ugupta@udel.edu

1. Introduction

Complex reaction networks are prevalent in numerous chemical and biochemical reaction systems [1], such as combustion [2], pyrolysis [3], catalytic conversion of hydrocarbons [4–6] and cell metabolism [7,8]. Microkinetic modeling is an essential step towards understanding design, optimization, and control of these systems. Although simulating the underlying system of governing equations, including ordinary differential equations (ODEs), algebraic equations (AEs), or differential–algebraic equations (DAEs), of a microkinetic model has become computationally cheap in recent years, achieving in-depth understanding of these networks is, however, limited. The ability to process the large amounts of data generated by solving the governing equations and to draw conclusions about the elementary steps underlying the reaction mechanism remain challenging. Reaction Path Analysis (RPA) or Reaction Flux Analysis overcomes this limitation by identifying the dominant chemistry by post-processing the solution of a microkinetic model [9]. RPA can be thought as a data (reaction nodes and edges) compression method. RPA has been used in combustion [10], pyrolysis, fluid–chemistry interactions [11], biochemical systems [7,12], chemical vapor deposition processes [13] and several catalytic reaction mechanisms (e.g., [14–16]).

Another application of RPA entails mechanism reduction to enable systems tasks. Despite the massive gains in computing power, predictive computational fluid dynamics (CFD) codes can only handle relatively small chemical kinetics models. The same

* Corresponding author.
E-mail address: vlachos@udel.edu (D.G. Vlachos).

https://doi.org/10.1016/j.softx.2020.100442

limitation also applies to other systems tasks, such as techno-economic analysis, optimization, and control. These issues underscore that reaction network reduction is essential to enable such tasks. RPA of chemical reaction systems has been used for mechanism reduction (e.g., [9,17–20]). Yet, another application of RPA is in model refinement and parameter estimation. For example, microkinetic modeling of complex reaction networks utilizes semi-empirical correlations like group additivity (GA), Brønsted–Evans–Polanyi (BEP), and linear scaling relations (LSR) for computational efficiency. The predictions of these correlations possess errors stemming from Density Functional Theory (DFT) calculations and parameter fitting [21]. The key reaction pathways along with possible rate determining steps (RDS) in the network, identified via RPA, can be refined through more accurate DFT calculations or parameter estimation from experimental data.

Most of the earlier implementations of RPA have been in-house codes, generally integrated with an in-house chemical kinetics software. Cantera [22], an open-source chemical kinetics software, computes the kinetic, thermodynamic, and species transport properties of a reaction network and solves the kinetic model. It then generates reaction path diagrams using the output of Cantera's chemical kinetics module. RMG [23] generates kinetic models composed of elementary chemical reaction steps using information about the chemistry of the reaction system. One of the modules in RMG generates flux diagrams using solutions from either an RMG job or a Chemkin job. OpenSMOKE^{++} [24] is a general framework for numerical simulations of reacting systems involving diffusion flames, combustion, and catalytic heterogeneous reactors. It utilizes the guidelines proposed in [11] to generate reaction path diagrams. GlycoVis [12] generates visualizations to show the distribution of glycans and potential reaction paths leading to each glycan in the N-Glycosylation network. The RPA visualization is, therefore, associated with a specific chemical kinetics software code or system alone. This motivates the development of a standalone, generic yet integrable reaction path visualizer with more functionalities.

The present manuscript demonstrates an automated, standalone, and generic RPA for complex reaction networks encountered in homogeneous or heterogeneous systems, including all reaction examples mentioned above. The python code employed uses the solution of a microkinetic model as an input and generates network and species visualizations that can be visualized in any internet browser or graphics editor. The methodology section discusses the different visualizations being generated by the visualizer. The application section presents demonstration of the visualizer for select complex reaction systems. The visualizations demonstrate the normalizations employed. One application shows the basic input files needed and another demonstrates the efficacy of the visualizer for large reaction networks.

2. Methodology

The reaction path visualizer takes in as input a list of species and reactions, defining the reaction network, along with a solution of the microkinetic model. This involves the reaction rates (both forward and reverse) and surface coverages of intermediates for a single or multiple reactor operating conditions. The quantities for identifying the important reactions and species and visualizing the dominant pathway include (1) the net rate of reaction, (2) the partial equilibrium index (PEI) [9], and (3) the relative importance of each reaction in the formation or consumption of each species. If unspecified, the PEI for each reaction is defined as

$$PEI = \frac{r_{forward}}{r_{forward} + r_{reverse}} \tag{1}$$

where $r_{forward}$ and $r_{reverse}$ are the absolute values of the forward and reverse reaction rates of a reaction, respectively. Note that PEI is dimensionless. The PEI is a measure of the degree of reversibility or distance from equilibrium of a reaction. Specifically, forward and reverse reaction rates are nearly equal for reactions being in partial equilibrium. A value close to 0.5 implies that reaction is in partial equilibrium while the entire reaction network may be far from equilibrium. Values close to 0 or 1 imply that the reaction is irreversible in the reverse or forward direction, respectively. Partially equilibrated reactions are typically fast in both directions, define a fast manifold constraining thermodynamically the species participating in a reaction, and are not RDS. In a reduced network, these reactions could potentially be left out as they are kinetically irrelevant but maybe thermodynamically important as they dictate concentrations of intermediates. Reactions far from partial equilibrium are potentially kinetically relevant, unless they are part of a slow reaction subnetwork occurring in parallel with the main pathways. One or more of these irreversible reactions determine the RDS.

Other inputs essential for the visualizer are defined below:

1. **Reaction rate cutoff** — Uses a float variable. This is used to refine the reaction network to be visualized. Any reaction with a net rate below the reaction rate cutoff is left out from the visualization but is not removed from the reaction network. The units is the same as that for the reaction rates.
2. **Equilibrium tolerance** — Uses a float variable between 0–0.5 to identify reactions that are in partial equilibrium. The value denotes the deviation in PEI value from partial equilibrium value of 0.5. The default value for this variable is taken to be 0.05. Any reaction with a PEI between 0.45 and 0.55 (0.05 $\pm$ equil. tol.) is considered to be in partial equilibrium.
3. **Visualization elements** — These include a set of elements present in the species molecular formula. Any species having at least one of the specified elements is considered in the visualization. In cases where the species names do not contain the molecular formula or the SMILES string, the elemental composition allows identifying molecules that contain a specific group of elements.

The above defined inputs enable trimming the reaction network (do not display kinetically insignificant reactions and species) making it easier to visualize and analyze. The reaction rate cutoff and visualization elements allow refinement in the number of edges and nodes considered in the visualization, respectively. The features of the visualizer are demonstrated using an example reaction network of ethanol steam reforming on Pt(111) surface. The microkinetic model has been taken from the literature [25] consisting of 67 species and 162 reactions. The input files can be accessed on the GitHub repository.

The visualizer generates a graph representation of the reaction network containing nodes representing species and edges representing reactions. The nodes are labeled using the defined species name. The edge thickness depicts the reaction flux within the reaction network between two species presenting the underlying dominant chemistry. The net rate of a reaction defines the direction of the arrow. The visualizer classifies reactions into partially equilibrated or not as well as surface and gas-phase reactions through different colors for easier identification. The edges are divided into three classes:

(1) Equilibrated reactions – Represented in green color
(2) Gas-phase reactions – Represented in red color
(3) Surface reactions – Represented in black color

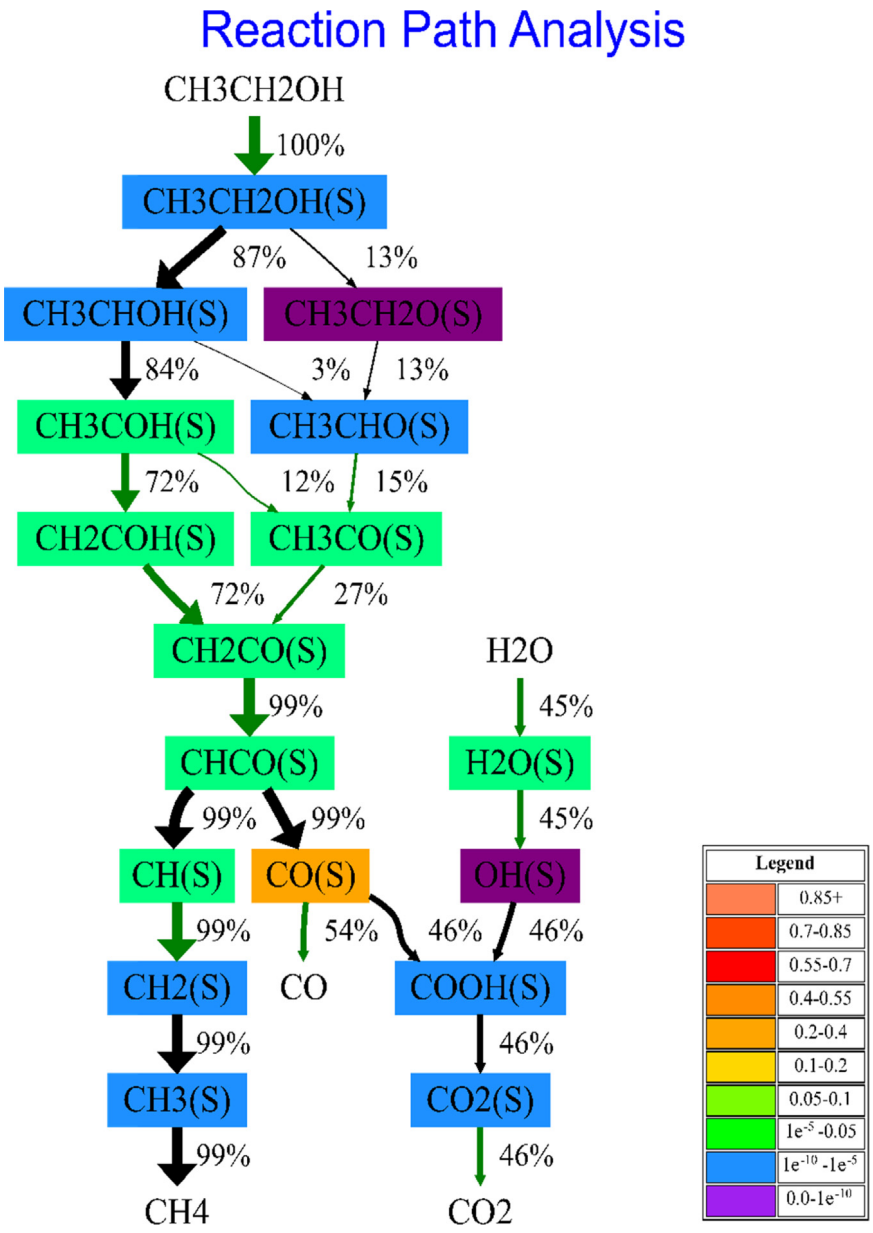

Fig. 1. Visualization using results from a microkinetic model of ethanol reforming on Pt. The node colors are based on the intermediates surface coverage shown in the legend. The node label denotes the species name used in the kinetic model. The nodes depicting gas-phase species are not colored. The edges represent partially equilibrated reactions in green and non-equilibrated surface reactions in black. The thickness of the edges is based on the net rate of initial reactant normalization. The percentages reflect the molar selectivity to different species with respect to the initial reactant in this example. The percentages may not sum to 100% due to round off error and/or minor paths not shown. The overall reaction is $C_2H_5OH + H_2O \rightarrow CH_4 + CO_2 + 2H_2$. The selectivity, however, is defined by the reaction rates. The coefficients based on selectivity has been specified in the Supporting Information (Fig. S.1). Note that these are specific to the reactor operating conditions. (For interpretation of the references to color in this figure legend, the reader is referred to the web version of this article.)

The python code generates an input file containing the species and network connectivity information which is passed as input to Graphviz [26], an open-source graph visualization software, to generate a visual representation of the reaction network. Graphviz contains a set of common graph layout algorithms. We use the *dot* algorithm that generates a ranked layout of a graph. The algorithm uses *mincross* that rearranges nodes within ranks to reduce edge crossings.

Multiple normalization methods have been implemented for analysis. The thickness of each edge is also set based on these normalized reaction rates.

(1) **Inlet reactant net-rate** (reactant-based) — This method normalizes the net rate of reactions with respect to the net rate of the reactant at inlet conditions.

$$Edge\ label,\ e_i = \frac{Net\ reaction\ rate,\ r_i}{\sum_{j=1}^{n} r_j} * 100\% \tag{2}$$

where n denotes the number of reactions the reactant is involved in and r_i denotes the reaction flux of reaction i. This quantity is again dimensionless.

The edges in the normalization shown in Fig. 1 represent the relative rate of a reaction with respect to the net rate of the initial reactant. The percentages provide the molar selectivity to different species with respect to the initial reactant. For example, a 99% value for CH_4 implies that for each mole of ethanol reacting, one mole of methane is generated. Similarly, the corresponding formation of CO and CO_2 is 0.54 mole and 0.46 mole, respectively.

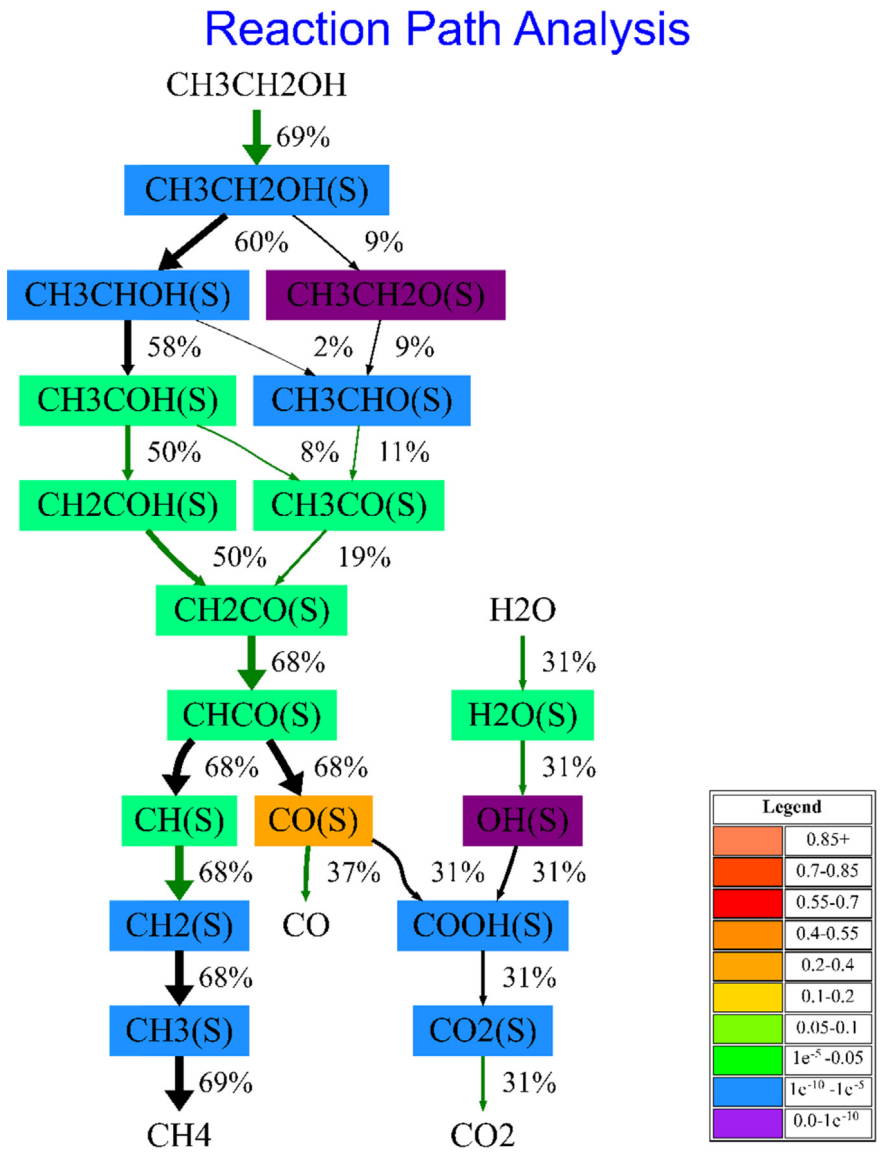

Fig. 2. Visualization using results from a microkinetic model of ethanol reforming on Pt. The thickness of the edges is based on the maximum rate in the reaction network normalization.

The CO/CO_2 ratio is controlled by the water-gas shift reaction network. It is to be noted that the above normalization is different from the directed relation graph method [27], where the interaction coefficient between a target species (initial reactant) and an intermediate defines if the intermediate needs to be considered in the reduced mechanism. This approach allows one to follow the flux of specific heteroatom, e.g., carbon, nitrogen, etc. from reactant(s) to product(s).

The arrows indicate a number of equilibrated steps (in green) and irreversible steps (in black), e.g., the first two dehydrogenations, the C–C cracking in the sufficiently dehydrogenated species CHCO, the hydrogenations of CH_2 to CH_4, and the formation of carboxyl from CO and OH and its conversion to CO_2. Ethanol, water, CO, and CO_2 are partially equilibrated with their gas-phase counterparts, but methane is not.

(2) **Maximum net reaction rate-based** — This method normalizes the net rate of the reactions with respect to the maximum reaction rate $r_{maxrate}$ in the network.

$$Edge\ label,\ e_i = \frac{Net\ reaction\ rate,\ r_i}{r_{\max rate}} * 100\% \tag{3}$$

In heterogeneous catalysis, the reaction rate is a function of both surface coverages of intermediates and the rate constant and therefore, the reaction rate of an intermediate can be higher than the *net rate* of the reactant. The maximum reaction rate provides an upper bound for normalization of reaction rates. The edge label is dimensionless.

The edges shown in Fig. 2 represent the relative rates with respect to the maximum one in the network. No edge corresponds to 100% because the maximum reaction rate is for hydrogen desorption, not considered here since the visualization elements used are only C and O. The complete visualization is shown in the Supporting Information (Fig. S.2).

(3) **Individual species consumption-based normalization** – If unspecified, the relative importance of each reaction in the consumption of each species is calculated.

$$Local\ consumption\ of\ reaction\ r_{i,S} = \frac{r_i}{\sum_{j=1}^{m} r_j} * 100\% \tag{4}$$

where $r_{i,S}$ is the percentage consumption of species S in reaction r_i, m is the number of reactions consuming species S. The local consumption of each species to different products is calculated

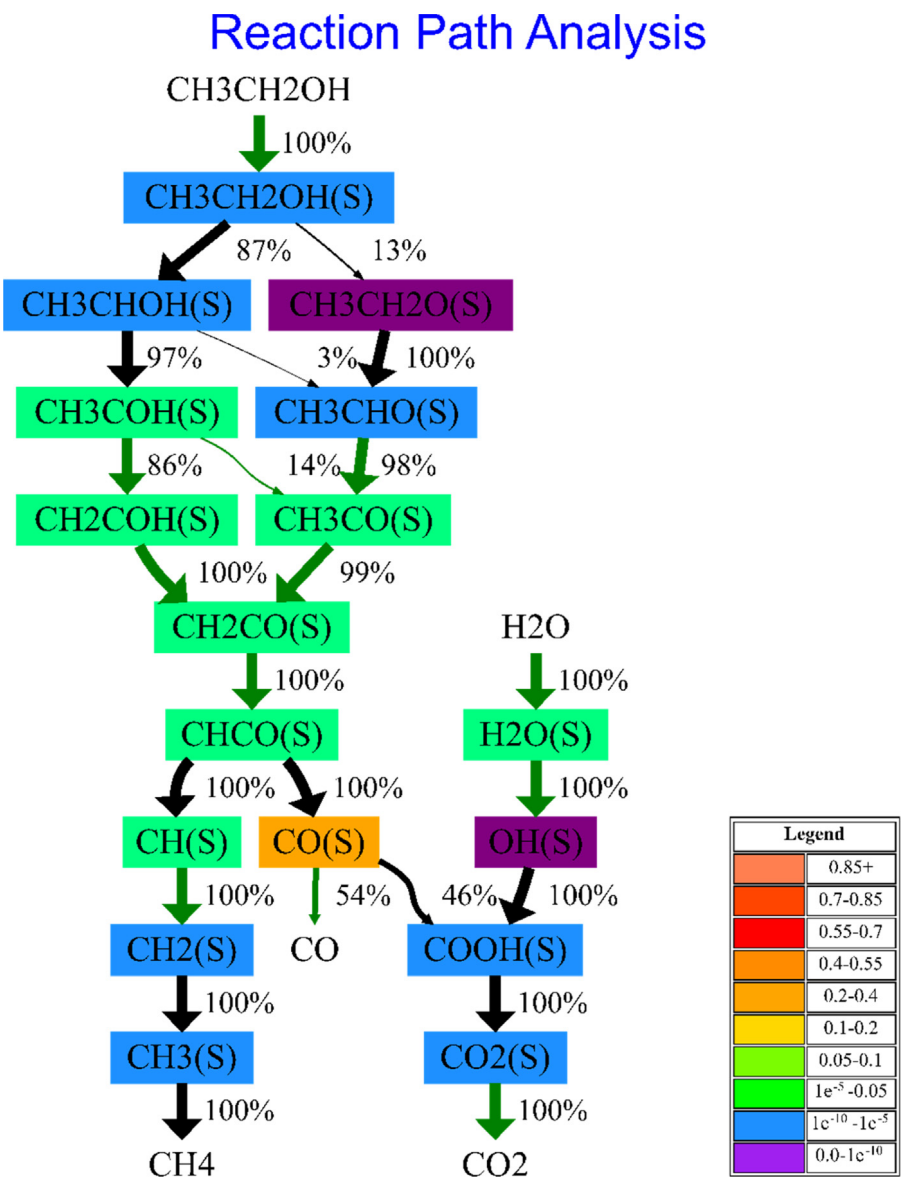

Fig. 3. Visualization using results from a microkinetic model of ethanol reforming on Pt. The thickness of the edges reflects the fraction of each species consumption normalization.

and the thickness of the edge reflects this. The visualization is shown in Fig. 3. The relative importance is again dimensionless.

An edge connecting species in Fig. 3 represents the percentage consumption of a species (left hand side of an elementary reaction) to other species (right hand side species). For example, 54% of the node "CO(S)", representing a CO molecule on the surface, desorbs to gaseous CO and 46% reacts with an OH(S) to form COOH(S). The visualization provides a local, species specific analysis compared to global analysis in the previous normalizations.

Each node in the above overall reaction network can be clicked to zoom in on the species visualization that shows the reactions that the species participates in. The species visualizations present reaction fluxes relevant to the species being examined. It is different from the reaction network visualizations discussed above where the entire network is visualized. For example, upon clicking on "CH3CHOH(S)" shown in any of the above visualizations, Fig. 4 is generated. Nodes that generate the selected species are on the left and nodes generated by the selected species on the right of the scheme. For equilibrated (non-equilibrated) reactions, we specify in order of appearance (1) the reaction number, (2) the percentage of production/consumption of this species by this specific reaction, (3) the equilibrium constant (net rate) for the specific reaction, and (4) the PEI. The user can traverse along the dominant reaction pathway by just clicking on the important species in the visualization. As an example, $CH_3CHOH(S)$ is generated exclusive (100%) from the adsorbed ethanol $CH_3CH_2OH(S)$ by dehydrogenation on the alpha carbon at a net rate of $4.8^{*}10^{-6}$ mol/s. The elementary reaction label is 16 and is fully irreversible (PEI = 1.00). Furthermore, $CH_3CHOH(S)$ is consumed mainly (∼96.8%) by further dehydrogenation to $CH_3COH(S)$ and H(S) with a rate of $4.6^{*}10^{-6}$ mol/s via reaction 17 which is close but not equilibrated (PEI = 0.56). The PEIs indicate that reaction 16, being farther from equilibrium compared to reaction 17, is potentially the RDS. A small fraction (3.2%) of $CH_3CHOH(S)$ is consumed to $CH_3CHO(S)$ and H(S) via reaction 71 that is partially equilibrated. These dehydrogenation steps require a second site of Pt, also depicted in the visualization.

Although the normalizations and visualizations look different in each case, the underlying dominant pathway is same and can be identified by following the thick edges starting from the initial

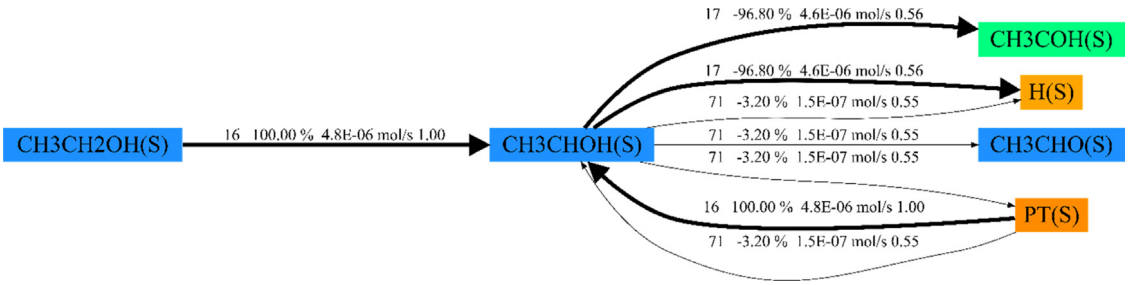

Fig. 4. Species visualization for CH3CHOH(S) showing elementary reactions forming and consuming it. The nodes are colored based on their surface coverages. The node labels represent the species name. The edge labels include (1) the reaction number, (2) production/consumption of CH3CHOH(S) species, (3) net reaction rate of the reaction, and (4) the partial equilibrium index..

Table 1
Species input for the visualizer. The entries involve species name, phase, and elemental composition of species. RU stands for the catalyst name and S1 in parenthesis means that the species is adsorbed.

Species_name	Species_phase	N	H	RU
H2	Gas	0	2	0
N2	Gas	2	0	0
NH3	Gas	1	3	0
RU(B)	Surface	0	0	1
RU(S1)	Surface	0	0	1
N2(S1)	Surface	2	0	0
N(S1)	Surface	1	0	0
H(S1)	Surface	0	1	0
NH3(S1)	Surface	1	3	0
NH2(S1)	Surface	1	2	0
NH(S1)	Surface	1	1	0

reactant. The implemented code is a standalone code integrable with any other kinetic code.

3. Applications

The efficacy of the reaction path visualizer is shown via its application on two complex reaction networks. The input files required for the visualizer are shown for an ammonia synthesis reaction system. The efficacy of the visualizer for large reaction networks is demonstrated using *p*-cresol hydrodeoxygenation reaction system.

3.1. Ammonia synthesis

The visualizer requires two input files — species.txt and reactions.txt. Table 1 shows the species file entries needed. The species name is used for node labeling. The phase and elemental composition information is used for node coloring and node refinement.

Table 2 shows the reactions file entries needed. The forward, reverse, and net reaction rates are used to calculate the edge thickness and arrow size. The partial equilibrium index is used for edge coloring and the reaction string is processed to identify the connections between different species in the reaction network.

The visualizer generates the visualization using the net rate of the reactant normalization shown in Fig. 5. It is clear that the first dehydrogenation from NH3(S1) and the 2N(S1) association to N2(S1) are kinetically relevant. The python code employed can be adapted to the user's inputs. For example, the node colors in Fig. 5 do not represent the surface coverages of species since the coverages were not provided by the user. The gas phase and surface species are shown with light brown and light blue colors, respectively, per user specification. The partial equilibrium index input is optional (the python code estimates it). The input files contain basic information about the reaction network that can be easily generated by any chemical kinetic software, making the visualizer applicable to any reaction system.

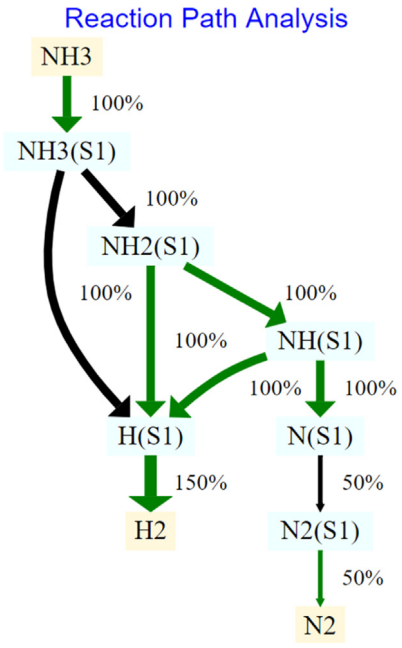

Fig. 5. Visualization generated using species and reactions inputs. The node colors are based on the phase: gas-phase species are colored in light brown and surface species in light blue. The node label denotes the species name used in the kinetic model. The thickness of the edges reflects the net rate based on reactant; one molecule of NH_3 ends up to 0.5 molecules of N_2 and 1.5 molecules of H_2. The overall reaction is $NH_3 \rightarrow 0.5N_2 + 1.5H_2$.

3.2. p-cresol hydrodeoxygenation (HDO)

Gu et al. studied the hydrodeoxygenation (HDO) of *p*-cresol [28] consisting of 183 species and 500 reactions. Their microkinetic model was in good agreement with two experimental data sets [29,30]. The dominant product in the two experimental cases was methylcyclohexanone (MCHO) in Nie's data and toluene (TOL) in Foster's data. The reason was attributed to be the varying space velocity. RPA using inlet reactant net-rate normalization at contact times of $W/F = 2$ gh/mol and 13 gh/mol, is shown in Figs. 6a and 6b, respectively. The species names were taken from the microkinetic model. The input files can be accessed on the GitHub repository. MCHO is the dominant product with 55% molar selectivity for short contact times and TOL is dominant with 86% molar selectivity for the longer contact time. In-depth analysis of this switch in dominant species was conducted by Gu et al. As demonstrated here, the RPA provides quick understanding about the dominant pathways and how these change with operating conditions.

Table 2
Reactions input for the visualizer. The entries involve forward, reverse, and net reaction rate, partial equilibrium index, and reaction string.

Fwd_rate	Rev_rate	Net_rate	PEI	Reaction_string
4.99E−01	4.99E−01	−3.51E−08	5.00E−01	H2 + 2 RU(S1) ↔ 2 H(S1) + 2 RU(B)
8.07E−02	8.07E−02	−1.17E−08	5.00E−01	N2 + RU(S1) ↔ N2(S1) + RU(B)
5.49E−01	5.49E−01	2.34E−08	5.00E−01	NH3 + RU(S1) ↔ NH3(S1) + RU(B)
2.50E−08	1.57E−09	2.34E−08	9.41E−01	NH3(S1) + RU(S1) ↔ H(S1) + NH2(S1) + RU(B)
6.11E−06	6.09E−06	2.34E−08	5.01E−01	NH2(S1) + RU(S1) ↔ H(S1) + NH(S1) + RU(B)
3.15E−04	3.15E−04	2.34E−08	5.00E−01	NH(S1) + RU(S1) ↔ H(S1) + N(S1) + RU(B)
6.93E−14	1.17E−08	−1.17E−08	5.92E−06	N2(S1) + RU(S1) ↔ 2 N(S1) + RU(B)

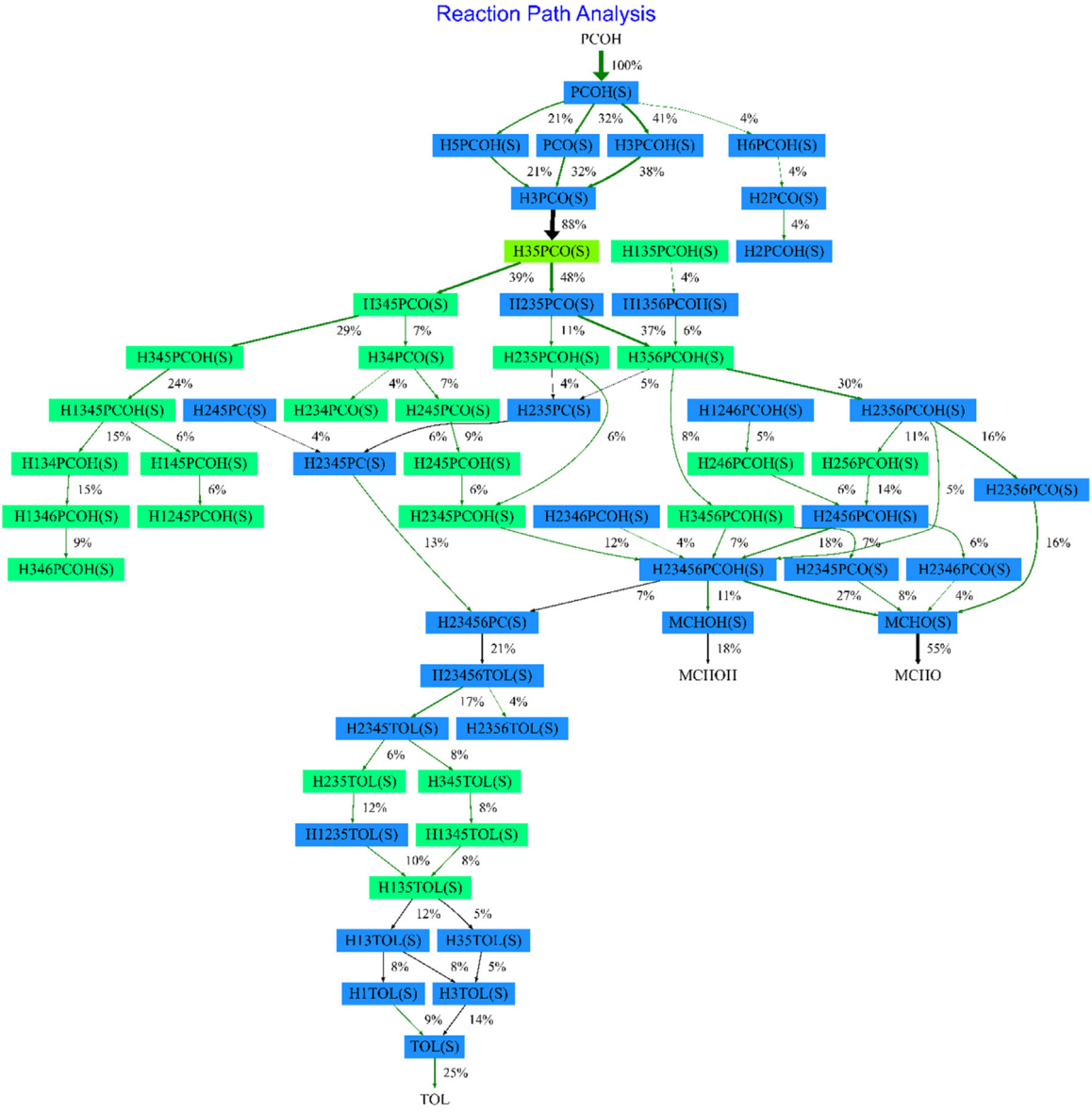

Fig. 6a. Reaction Network Visualization for HDO of p-cresol using inlet reactant net-rate normalization at short contact times of $W/F = 2$ gh/mol. The node labels represent species names taken from the microkinetic model. MCHO (methylcyclohexanone) is the dominant product with molar selectivity of 55%. The network involves several overall reactions (not shown). The dominant one is p-cresol + $2H_2$ → MCHO.

4. Conclusions

An open-source, standalone reaction path visualizer software, the ReNView, has been implemented and demonstrated for visualization of reaction networks and species. The features and input/output information for the visualizer have also been discussed. The efficacy and flexibility of the visualizer has been shown through case studies. Input parameters allow control of the visualized reaction network. Multiple normalizations were presented to demonstrate the potential of the visualizer in identifying the dominant underlying chemistry.

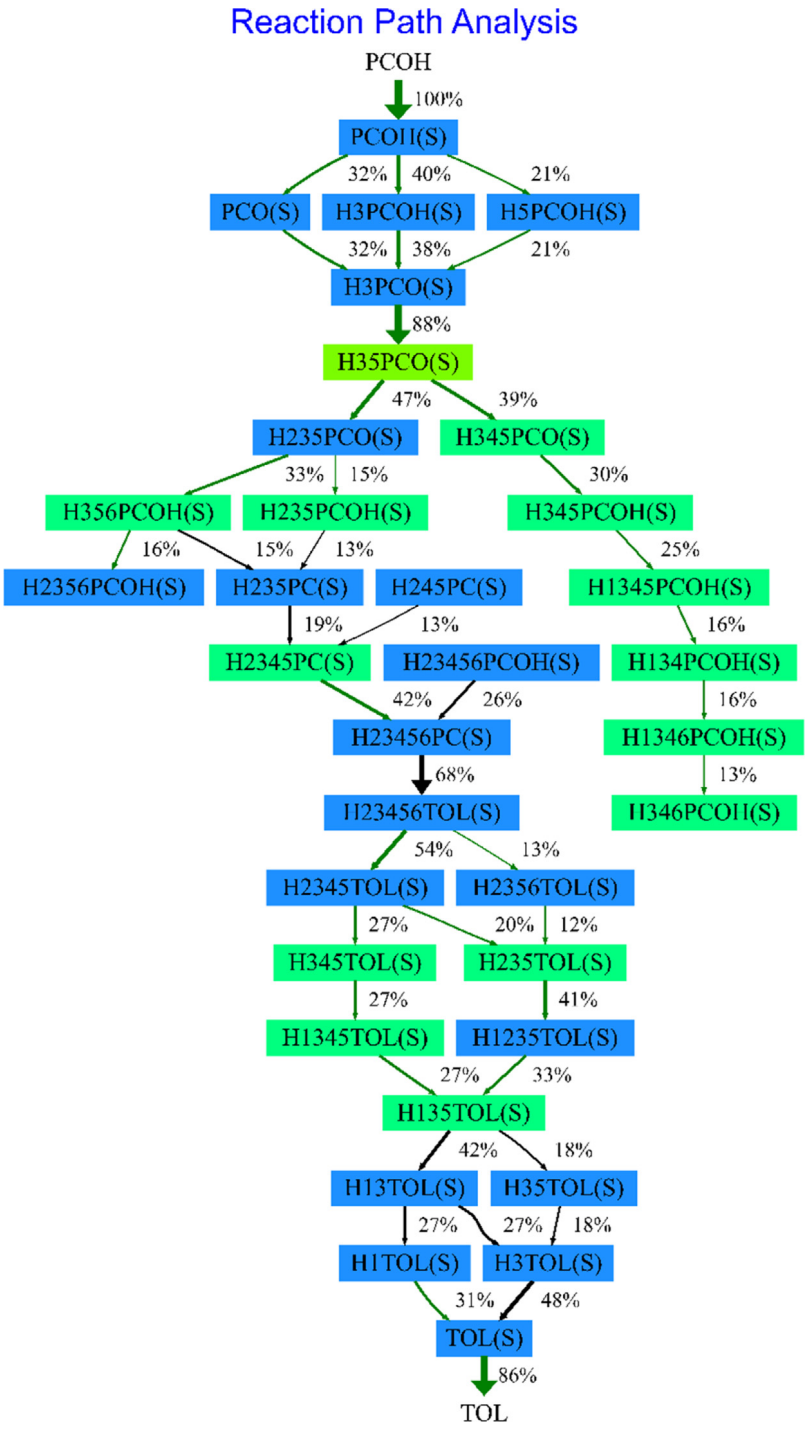

Fig. 6b. Reaction Network Visualization for HDO of p-cresol using inlet reactant net-rate normalization at contact time of $W/F = 13$ gh/mol. The node labels represent species names taken from the microkinetic model. TOL (toluene) is the dominant product with molar selectivity of 86%.

Declaration of competing interest

The authors declare that they have no known competing financial interests or personal relationships that could have appeared to influence the work reported in this paper.

Acknowledgments

This work was supported in part by the RAPID manufacturing institute, USA, supported by the Department of Energy (DOE) Advanced Manufacturing Office (AMO), award number DE-EE0007888-9.5. RAPID projects at the University of Delaware are also made possible in part by funding provided by the State of Delaware. The Delaware Energy Institute gratefully acknowledges the support and partnership of the State of Delaware in furthering the essential scientific research being conducted through the RAPID projects. We would also like to thank Gerhard Wittreich, Hilal Ezgi Toraman and Jonathan Lym for testing the visualizer and providing feedback.

Appendix A. Supplementary data

Supplementary material related to this article can be found online at https://doi.org/10.1016/j.softx.2020.100442.

References

[1] Broadbelt LJ, Pfaendtner J. Lexicography of kinetic modeling of complex reaction networks. AIChE Journal 2005;51(8):2112–21. http://dx.doi.org/10.1002/aic.10599.

[2] Battin-Leclerc F, Blurock E, Bounaceur R, Fournet R, Glaude PA, Herbinet O, et al. Towards cleaner combustion engines through groundbreaking detailed chemical kinetic models. Chem Soc Rev 2011;40(9):4762–82.

[3] Froment GF, Van de Steene BO, Van Damme PS, Narayanan S, Goossens AG. Thermal cracking of ethane and ethane-propane mixtures. Ind Eng Chem Process Des Dev 1976;15(4):495–504.

[4] Laxmi Narasimhan CS, Thybaut JW, Marin GB, Denayer JF, Baron GV, Martens JA, et al. Relumped single-event microkinetic model for alkane hydrocracking on shape-selective catalysts: Catalysis on ZSM-22 pore mouths, bridge acid sites and micropores. Chem Eng Sci 2004;59(22–23):4765–72.

[5] Corma A, Huber GW, Sauvanaud L, P.O. Connor. Biomass to chemicals: Catalytic conversion of glycerol/water mixtures into acrolein, reaction network. J Catal 2008;257:163–71.

[6] Rangarajan S, Bhan A, Daoutidis P. Rule-based generation of thermochemical routes to biomass conversion. Ind Eng Chem Res 2010;49(21):10459–70.

[7] Gupta U, Le T, Hu W-S, Bhan A, Daoutidis P. Automated network generation and analysis of biochemical reaction pathways using RING. Metabolic Engineering 2018;49:84–93.

[8] Le T, O'Brien C, Gupta U, Sousa G, Daoutidis P, Hu WS. An integrated platform for mucin-type O-glycosylation network generation and visualization. Biotechnol Bioeng 2019;116:1341–54.

[9] Salciccioli M, Stamatakis M, Caratzoulas S, Vlachos DG. A review of multiscale modeling of metal-catalyzed reactions: Mechanism development for complexity and emergent behavior. Chem Eng Sci 2011;66(19):4319–55.

[10] Pfaendtner J, Broadbelt LJ. Mechanistic modeling of lubricant degradation. 2. the autoxidation of decane and octane. Ind Eng Chem Res 2008;47(9):2897–904.

[11] Grcar JF, Day MS, Bell JB. Conditional and opposed reaction path diagrams for the analysis of fluid-chemistry interactions. 2003;.

[12] Hossler P, Goh LT, Lee MM, Hu WS. GlycoVis: Visualizing glycan distribution in the protein N-glycosylation pathway in mammalian cells. Biotechnol Bioeng 2006;95(5):946–60.

[13] Salami H, Ramakrishnasubramanian K, Adomaitis RA. Reaction path analysis for chemical vapor deposition and atomic layer deposition processes: A study of titania thin-film deposition. Phys Status Solidi Basic Res 2017;254(10).

[14] Salciccioli M, Chen Y, Vlachos DG. Microkinetic modeling and reduced rate expressions of ethylene hydrogenation and ethane hydrogenolysis on platinum. Ind Eng Chem Res 2011;50(1):28–40. http://dx.doi.org/10.1021/ie100364a.

[15] Mhadeshwar AB, Vlachos DG. Is the water-gas shift reaction on Pt simple? Computer-aided microkinetic model reduction, lumped rate expression, and rate-determining step. Catal Today 2005;105:162–72.

[16] Deshmukh SR, Mhadeshwar AB, Vlachos DG. Microreactor modeling for hydrogen production from ammonia decomposition on ruthenium. Ind Eng Chem Res 2004;43(12):2986–99. http://dx.doi.org/10.1021/ie030557y.

[17] Sun W, Chen Z, Gou X, Ju Y. A path flux analysis method for the reduction of detailed chemical kinetic mechanisms. Combust Flame. 2010;157(7):1298–307. http://dx.doi.org/10.1016/j.combustflame.2010.03.006.

[18] Raimondeau S, Gummalla M, Park YK, Vlachos DG. Reaction network reduction for distributed systems by model training in lumped reactors: Application to bifurcations in combustion. Chaos. 1999;9(1):95–107.

[19] Gupta U, Heo S, Bhan A, Daoutidis P. Time scale decomposition in complex reaction systems: A graph theoretic analysis. Comput Chem Eng 2016;95:170–81. http://dx.doi.org/10.1016/j.compchemeng.2016.09.011.

[20] Susnow RG, Dean AM, Green WH, Peczak P, Broadbelt LJ. Rate-based construction of kinetic models for complex systems. J Phys Chem A 1997;101(20):3731–40.

[21] Sutton JE, Vlachos DG. Error estimates in semi-empirical estimation methods of surface reactions. J Catalysis 2013;297:202–16. http://dx.doi.org/10.1016/j.jcat.2012.10.009.

[22] Goodwin David G, Moffat K, Speth RL. Cantera: an object-oriented software toolkit for chemical kinetics, thermodynamics, and transport processes. 2016, http://dx.doi.org/10.5281/zenodo.45206.

[23] Gao CW, Allen JW, Green WH, West RH. Reaction mechanism generator: Automatic construction of chemical kinetic mechanisms. Comput Phys Comm 2016;203:212–25.

[24] Cuoci A, Frassoldati A, Faravelli T, Ranzi E. OpenSMOKE++: An object-oriented framework for the numerical modeling of reactive systems with detailed kinetic mechanisms. Comput Phys Comm 2015;192:237–64.

[25] Sutton JE, Panagiotopoulou P, Verykios XE, D.G. Vlachos. Combined DFT microkinetic and experimental study of ethanol steam reforming on Pt. J Phys Chem C 2013;117(9):4691–706.

[26] Ellson J, Gansner E, Koutsofios L, North SC, Woodhull G. Graphviz— open source graph drawing tools. international symposium on graph drawing. 2002, p. 483–4, Available from: http://link.springer.com/10.1007/3-540-45848-4_57.

[27] Lu T, Law CK. A directed relation graph method for mechanism reduction. Proc Combust Inst 2005;30(1):1333–41. http://dx.doi.org/10.1016/j.proci.2004.08.145.

[28] Gu GH, Mullen CA, Boateng AA, Vlachos DG. Mechanism of dehydration of phenols on noble metals via first-principles microkinetic modeling. ACS Catal 2016;6(5):3047–55.

[29] Foster AJ, Do PTM, Lobo RF. The synergy of the support acid function and the metal function in the catalytic hydrodeoxygenation of m-cresol. Top Catal 2012;55(3–4):118–28.

[30] Nie L, Resasco DE. Kinetics and mechanism of m-cresol hydrodeoxygenation on a Pt/SiO_2 catalyst. J Catalysis 2014;317:22–9. http://dx.doi.org/10.1016/j.jcat.2014.05.024.